

Sensitivity analysis of a CCD-based camera system for the retrieval of bidirectional reflectance distribution function for vicarious calibration

Prabal Nandy, Kurt Thome, Stuart Biggar

Remote Sensing Group, Optical Sciences Center
University of Arizona
P.O. Box 210094, Tucson AZ 85721-0094
Phone:(520) 621-2158 Fax:(520) 621-8292
Email: nandy@opt-sci.arizona.edu

ABSTRACT

The University of Arizona, Optical Sciences Center, Remote Sensing Group is involved with the vicarious calibration of satellite sensors in support of NASA's Earth Observing System (EOS) program. Sensor calibration coefficients are calculated by comparing sensor DN values to top of the atmosphere (TOA) radiance values, calculated from radiative transfer code (RTC). The RTC output is based on measurements of site spectral reflectance and atmospheric parameters at a selected test site. The bidirectional reflectance distribution function (BRDF) which relates the angular scattering of a given beam of incident radiation on a surface, is an important factor in these radiative transfer calculations. The inclusion of BRDF data into RTC calculations improves the level of accuracy of the vicarious calibration method by up to 5% over some target sites. BRDF data is also valuable in the validation of Multi-Angle Imaging Spectroradiometer (MISR) data sets.

The Remote Sensing Group has developed an imaging radiometer system for ground-based measurements of BRDF. This system relies on a commercially-available 1024- by 1024-pixel silicon CCD array. Angular measurements are accomplished with a 8-mm focal length fisheye lens that has a full 180-degree field of view. Spectral selection is through four interference filters centered at 470, 575, 660 and 835 nm, mounted internally in the fisheye lens. This paper discusses the effect of calibration errors in this camera system on the retrieval of Hapke/Jacquemoud surface parameters from modeled BRDFs. The effect of these retrieved BRDFs on vicarious calibration results is discussed. Data processing schemes for the retrieval of these parameters from BRDF camera data sets are described. Based on these calculations, calibration requirements for digital camera BRDF-retrieval systems are presented.

Keywords: BRDF, CCD, Reflectance, Vicarious Calibration, Digital Camera

1. INTRODUCTION

The bi-directional reflectance distribution functions (BRDF) of surfaces have been of interest for a wide variety of problems for some time. All surfaces, whether they are natural or artificial, are optically nonuniform at scales greater than the molecular, and hence scatter incident light.¹ Since the BRDF is an intrinsic quality of a material that relates the angular pattern of reflection from a surface to a given beam of incident radiation, it is of prime importance whenever the scattering of light occurs in nature.² Furthermore, it has been shown through studies of vegetation canopies and soils that most natural surfaces reflect light anisotropically, making the measurement of BRDF over a range of viewing and illumination geometries necessary.^{3,4}

The most basic application to require BRDF is the use of the function to characterize the radiation field leaving a surface as a result of incident solar radiation. Since all measurements of surfaces in the field occur with the sun at a particular illumination geometry, such reflectance measurements are inherently bidirectional in nature.⁵ The BRDFs of different surfaces can then be used in the normalization of wide-field and off-nadir satellite imagery of terrestrial surfaces, land cover classification, and cloud detection.⁶ The inclusion of BRDF data in this manner allows off-nadir

sampled data to be freed from directional effects, making the radiometric correction of wide-angle satellite imagery possible.^{5,7,8} BRDF information can then be used for the correction of surface BRDF effects in a time-series of satellite observations of a particular region.⁹ Such a use of BRDF has applications in global change studies, for example, where the long historical database of Advanced Very High Resolution Radiometer (AVHRR) data can be BRDF-corrected for the calculation of land cover change over a long period of time.¹⁰

Recent advances in digital camera technology have made commercially available charged-coupled-device (CCD) camera systems an attractive alternative to mechanical goniometric systems for BRDF retrieval.¹¹ CCD cameras, which use a large number of discrete detectors arranged in a 2-D array structure, have the implicit advantage over conventional non-imaging systems in that an entire set of angular measurements can be made simultaneously, without the need for mechanical rotation of the detector elements. This ability to sample over many nadir and azimuth angles at once allows BRDF to be retrieved with less need for the interpolation between measurements than has been previously required.¹²

The Remote Sensing group of the Optical Sciences Center at the University of Arizona has been involved in the collection of data for the vicarious calibration of Earth-observing satellites since the early 1980s. As part of these vicarious calibrations, (TOA) radiance in the visible, near and shortwave infrared is predicted through the use of atmospheric models and radiative transfer codes. These codes are provided with parameters derived from on-site measurements of surface reflectance and atmospheric conditions at the time of satellite overpass at a selected location.¹³ To calibrate the satellite sensor, this TOA radiance is then compared to the digital number (DN) produced by the instrument to compute radiometric gain coefficients for the detector. An important component of the surface reflectance model used by radiative transfer codes is the BRDF.¹⁴ In these codes, the BRDF of a surface represents the lower boundary condition for atmospheric radiative transfer. These radiative transfer models may then in turn be used to calculate the TOA radiance measured by optical satellites.¹⁵ The addition of the BRDF function into radiative transfer models is therefore expected to improve the accuracy of predicted TOA radiance.¹⁶

The purpose of this study is to evaluate the requirements for, and the calibration of an imaging CCD camera system for the retrieval of BRDF data for the improvement of vicarious calibration methods for remote sensing. The Remote Sensing Group has developed an imaging radiometer for ground-based measurements of BRDF.¹⁷ The BRDF camera system relies on a commercially-available, astronomical-grade 1024- by 1024-pixel, cooled silicon CCD array with 14-bit radiometric resolution. Angular measurements are accomplished using an 8-mm fisheye lens that has a full 180-degree field of view. Each pixel on the CCD array has a nominal 0.2 degree field of view. Spectral selection is through four interference filters centered at 470, 575, 660, and 835 nm mounted in a filter wheel internal to the fisheye lens. The system is designed such that the entire 180-degree field is collected at one time with an integration time on the order of a few seconds per band and a complete multispectral data set, including dark images, collected in under two minutes.

Scientific use of such an imaging system requires the individual calibration of the large number of detector elements that compose the 2-D CCD array. Gain and offset parameters for each pixel of the imaging array are then used to perform a pixel-by-pixel correction of data to allow pixel to pixel variations due to the detector to be removed from the data.¹⁸

This current work examines the sensitivity of BRDF retrieval techniques to simulated instrument noise and biases. Two models of soil BRDFs based on the parameterization of surface features were used to generate BRDF functions which were then randomly perturbed. Instrument calibration requirements for the CCD camera system were then determined by examining the effects of simulated noise and biases on the retrieval of surface reflectance parameters from the perturbed BRDF models. The retrieval methods used in this study are the same as those procedures as are used to process field data for the RSG.¹⁹

2. THEORY AND MODELS

In this study, two surface reflectance models that describe the BRDFs of soil surfaces consistent with the field use of the RSG's BRDF camera system were used to generate modeled BRDFs. These models were perturbed to simulate the effects of random noise and calibration errors in the BRDF camera system. The perturbed models were inverted with the same data processing routine performed on the RSG's field data sets, resulting in retrieved surface reflectance parameters. These parameters were then used to generate new BRDFs which were compared against the original models to evaluate the sensitivity of BRDF retrieval algorithms to errors in instrument calibration.

2.1 BRDF Models

In practice, the prohibitively large number of possible illumination and viewing geometries required to derive BRDF from empirical data necessitates the use of surface reflectance models to describe the properties of a given surface. These models generate a continuous BRDF for a variety of illumination and view geometries based on a small number of surface parameters. These parameters may be related to macroscopic physical properties of the surface, such as soil grain size and single-scatter albedo.²⁰ The parameters of a given surface model are usually derived by fitting the model to a small number of measured data points. The model is then used to interpolate between the measured values to generate a continuous BRDF function used in RTCs.¹² BRDF models have been used in this manner successfully to model various vegetated and bare soil surfaces in the field and from orbit for remote sensing applications for many years.^{9,20,21,22}

The two models considered in this study are the Hapke and the Walthall BRDF models.^{1,23} The Hapke model is a nine-parameter model based on simplified equations of radiative transfer. This model has been used in various forms in the field of remote sensing for the BRDF characterization of soils.²² The Walthall model, alternatively, is a simple three-parameter empirical formula designed to model the BRDF of soils and vegetation canopies, and has been used to successfully model the reflectances of various types of surfaces.²³ The Walthall model is a more recent BRDF model in comparison, which arose out of the need for a simple equation to fit the relatively large number of measurements produced by modern automated BRDF goniometer systems.²⁰ Both models are analyzed from the standpoint of a sensitivity analysis of the BRDF camera system's requirements and are presented here as examples of two general BRDF models.

2.1.1 The Hapke Model

The Hapke model makes nine major assumptions that are applicable to diffusely-reflective surfaces such as powders and soils similar to those imaged in this study. A discussion of the equations of radiative transfer involved in the derivation of the Hapke model can be found in Hapke's book on spectral reflectance¹.

The model proposed by Hapke taking into account both single-scatter and multiple-scatter terms is

$$f_r(\theta_i, \phi_i; \theta_r, \phi_r) = \frac{\omega_0}{4} \frac{1}{\mu_i + \mu_r} \times \{P(g, g') [1 + B(g)] + H(\mu_i)H(\mu_r) - 1\} \quad (1)$$

where f_r is the BRDF as a function of incident and reflected angles θ and ϕ respectively, ω_0 is the single scatter albedo, the ratio of scattered light to total incoming light, and μ_i and μ_r are the direction cosines of the incoming and outgoing light. The variable g is the phase angle, while, g' is defined as the angle between the specular reflection direction and view, as derived by Jacquemoud.²⁴ The function $P(g, g')$ is the average particle scattering phase function. In this work we use a modified version of the phase function which was derived from a second-order Legendre polynomial expansion by Pinty and Verstraete.²² This new function incorporates two new coefficients created by Jacquemoud to account for the forward scattering specular peak of soil targets and is defined as

$$P(g, g') = a + b \cos(g) + c \left[\frac{(3\cos^2(g) - 1)}{2} \right] + d \cos(g') + e \left[\frac{(3\cos^2(g') - 1)}{2} \right] \quad (2)$$

where b , c , d and e , are multipliers adjusted to provide the best fit to the phase function data.²⁴ The b and d coefficients define the slope of the fit in terms of g and g' respectively, while the c and e coefficients control the overall curvature of the phase function. The coefficient a is a simple offset term added for use in this study to improve the functional fit. The Jacquemoud equation reduces to the Pinty-Verstraete equation in the case where c and d equal 0 (i.e., no specular peak). This function assumes azimuthal symmetry about the principal plane and has been shown to produce good agreement with field data collected over soil targets, particularly those displaying a mix of forward and backscatter reflections.²⁴

The term $B(g)$ is defined as the backscattering function which accounts for the so-called 'opposition effect' which arises at small phase angles.²⁵ Hapke defines several forms of this equation, the one used here is the one shown

to produce good results for the modelling of soil targets by Pinty and Verstraete where h is the angular width of the backscatter peak, and B_0 is its amplitude expressed as

$$B_0 = \frac{S(0)}{\omega_0 P(0,0)} \quad (3)$$

where $S(0)$ is the fraction of light scattered by particles at the surface in the backscatter direction.²² $H(\mu)$ is Chandrasekhar's "H-Function".²⁶ This function is an integral that describes the angular pattern of emergent radiation from an infinite field of isotropic scatterers. The combined $[H(\mu_i) H(\mu_r) - 1]$ term in (1) accounts for the multiple scatter contribution of the BRDF function.²² The simple two-stream approximation to the H-function integral derived by Hapke is the one used in this work where μ is either μ_i or μ_r respectively.²⁵ From equation (1) it is clear that to fit a BRDF surface to Hapke's model, eight coefficients must be retrieved. These coefficients are the $a, b, c, d, e,$ parameters of the Jacquemoud phase function, the single-scatter albedo ω_0 , the backscatter angular width h , and the backscatter magnitude $S(0)$. In this work example BRDFs are modeled using typical values of these parameters for soil targets consistent with those from literature.

2.1.2 The Walthall Model

The Walthall model was proposed to describe the bidirectional reflectance of vegetative canopies and bare soil surfaces. The purpose of the surface-reflectance model was explicitly to provide a simple method for calculating the lower boundary condition for RTCs, and for studying the effects of BRDF on off-nadir imaging sensors. The model was designed empirically, based loosely on the limaçon of Pascal, modified to fit the observed BRDF of soil and vegetation surfaces. The model explicitly ignores phenomenon such as surface roughness, texture, shadowing, and other physical parameters.²³ The model proposed by Walthall is

$$f_r(\theta_i, \phi_i; \theta_r, \phi_r) = \alpha \theta_r^2 + \beta \theta_r \cos(\phi_r - \phi_s) + \gamma \quad (4)$$

where the $\alpha, \beta,$ and γ coefficients are adjusted to provide the best fit with the data. Physically the α coefficient controls the general surface curvature of the BRDF surface, the β coefficient provides the linear dependance on view zenith angle, and the γ term is a simple offset. Based on (4), the Walthall model assumes BRDF functions are symmetric about the principal plane in azimuth. This function has been used successfully to model the reflectance of soils and vegetation and has shown good agreement with data collected over various types of crops and levels of soil roughness.²³

3. SENSITIVITY ANALYSIS

The Hapke and Walthall models were used in this study as examples of the expected BRDFs retrieved by the RSG's BRDF camera system. BRDF surfaces were generated using the Hapke and Walthall models and using parameters taken from the literature for surfaces under different illumination conditions.

The models were then perturbed by both random noise, and linear 'tilt' bias errors, to simulate errors in the gain calibration and the lens system calibration respectively. This was done by multiplying the simulated BRDF at a particular illumination geometry by an error function. New surface parameters were retrieved from the perturbed model by minimizing the fit error between the perturbed BRDF and the model based on the new parameters as

$$\delta^2 = \sum_{k=1}^n [f_k - f(\theta_{ik}, \phi_{ik}; \theta_{rk}, \phi_{rk})]^2 \quad (5)$$

where δ is the fit error to be minimized over all data points, f is the modeled BRDF of the surface based on the new perturbed surface parameters, while f_k is the BRDF of the perturbed model.²²

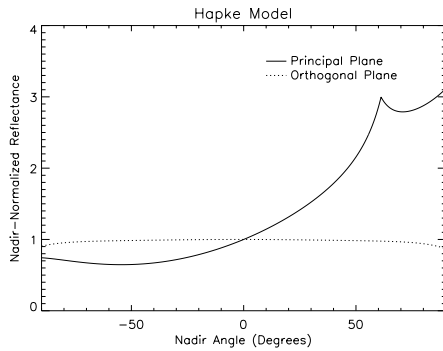


Figure 1: The Hapke model based on Jacquemoud's surface parameters for dry clay. +60 degrees is the backscatter direction.

deviation of 0.7%.²⁴ Modeled BRDF values were calculated using (6) for every 0.2-degrees in zenith and azimuth angles from -90 to 90 degrees with respect to nadir and from 0 to 360-degrees with respect to the solar principal plane. The nadir-view normalized reflectance generated by this model in the principal and orthogonal planes is shown in figure 1. This model will be referred to as the original Hapke model in this study. Most notable about this model is the backscatter peak seen at a viewing angle of +60 degrees in the principal plane, and the nearly lambertian reflectance of the surface in the orthogonal plane of the model.

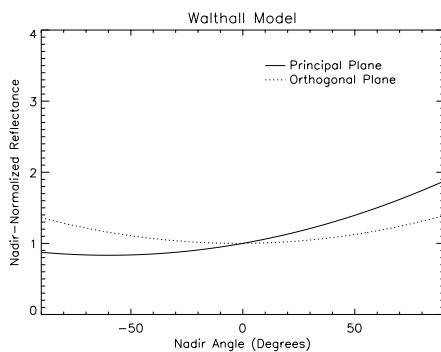


Figure 2: The Walthall model based on Walthall's surface parameters for a smooth gravel surface. +44 degrees is the backscatter direction.

distributed 5% and 10% random error function. These perturbed models were also multiplied by a 5% and 10% slope to simulate the effect of a miscalibration of the camera system. The eight resulting data sets are referred to as the 5% random, 10% random, 5% random and tilt, and 10% random and tilt, Hapke and Walthall perturbed models in this study.

Derived BRDF models were generated based on the data from these eight perturbed models to simulate BRDF retrieval from a miscalibrated instrument. This was done by inverting the perturbed models, using a two-dimensional Levenberg-Marquardt least-squares fitting routine. The routine was designed to minimize the error between the derived and perturbed models by minimizing the error (5), and was found to return all eight parameters of the Hapke model and the three parameters of the Walthall model to better than 0.001% in the case of the original unperturbed models, when given data from the principal and orthogonal planes of the modeled BRDF. This procedure was used to derive new surface reflectance parameters based on data taken from the perturbed model. This new set of parameters were then used to produce a derived model, which was ratioed against the original (unperturbed) model to see the effects of the random errors on BRDF retrieval. In all cases the derived model fit the perturbed data sets with better than a 2.9% standard deviation. The effect of the perturbations on the derived BRDF models were found to be greater in all cases in the principal planes of the data sets. The ratio between the derived and original model principal plane data sets for the Hapke and Walthall models, for the cases of the 5% random, 10% random, 5% random and tilt, and 10% random and tilt errors are shown in figures 3 through 6 respectively.

To determine the effect of uncorrected pixel-to-pixel gain variations on the retrieval of BRDF, a Hapke-Jacquemoud model was generated as an example soil surface. This BRDF was created using (1) and the Jacquemoud phase function (2). The surface reflectance parameters used to generate the model were those of a clay soil sample measured by a goniometer in the laboratory, illuminated with a lamp at a zenith angle of 60 degrees and a wavelength of 538 nm by Jacquemoud.²⁴ In this model, the a , b , c , d , e , parameters of the modified Jacquemoud phase function are set to 1.0, 1.665, 0.864, 0.357, and 0.041 respectively, the single-scatter albedo ω_0 is set to 0.363, and the backscatter angular width h , and magnitude $S(0)$ are set to 0.101 and 1.0 respectively. These parameters were found by Jacquemoud to fit his experimental data with a standard

A Walthall BRDF model was also generated for this study, based on surface parameters derived from data collected over a smooth gravel surface at a wavelength of 550 nm by Walthall.²³ The α , β , and γ parameters for this surface illuminated at a solar angle of 44 degrees are 1.09, 2.24, and 6.88 respectively, and were found to fit Walthall's experimental data with a standard deviation of 5.5%. The nadir-view normalized reflectance for the original Walthall BRDF model in the principal and orthogonal planes is shown in figure 2. The BRDF of this surface is lower than that of the Hapke model in the principal plane backscattering direction, but higher at larger viewing angles in the orthogonal plane.

To simulate the effect of instrument noise and gain nonuniformity on the retrieval of BRDF data, both models were perturbed by multiplying them with a uniformly-

distributed 5% and 10% random error function. These perturbed models were also multiplied by a 5% and 10% slope to simulate the effect of a miscalibration of the camera system. The eight resulting data sets are referred to as the 5% random, 10% random, 5% random and tilt, and 10% random and tilt, Hapke and Walthall perturbed models in this study.

Derived BRDF models were generated based on the data from these eight perturbed models to simulate BRDF retrieval from a miscalibrated instrument. This was done by inverting the perturbed models, using a two-dimensional Levenberg-Marquardt least-squares fitting routine. The routine was designed to minimize the error between the derived and perturbed models by minimizing the error (5), and was found to return all eight parameters of the Hapke model and the three parameters of the Walthall model to better than 0.001% in the case of the original unperturbed models, when given data from the principal and orthogonal planes of the modeled BRDF. This procedure was used to derive new surface reflectance parameters based on data taken from the perturbed model. This new set of parameters were then used to produce a derived model, which was ratioed against the original (unperturbed) model to see the effects of the random errors on BRDF retrieval. In all cases the derived model fit the perturbed data sets with better than a 2.9% standard deviation. The effect of the perturbations on the derived BRDF models were found to be greater in all cases in the principal planes of the data sets. The ratio between the derived and original model principal plane data sets for the Hapke and Walthall models, for the cases of the 5% random, 10% random, 5% random and tilt, and 10% random and tilt errors are shown in figures 3 through 6 respectively.

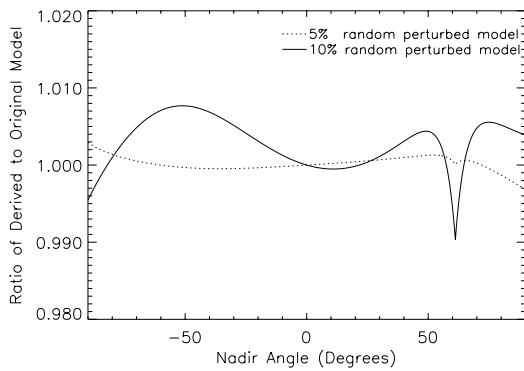


Figure 3: Ratio of derived Hapke model to original with 5% and 10% random error.

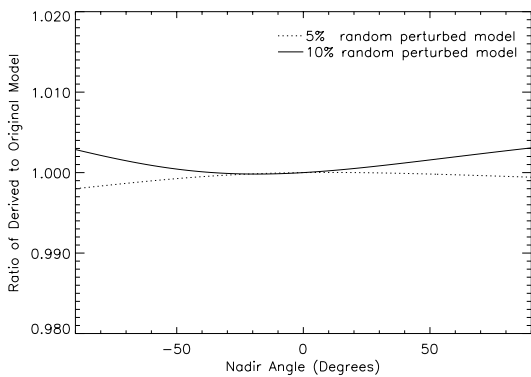


Figure 4: Ratio of derived Walthall model to original with 5% and 10% random error.

gain miscalibration would cause at most a 2% error in the BRDF retrieved at large view angles near the backscattering peak, with less than a 1% error everywhere else. For a miscalibration on the order of 5%, this error drops to less than 0.5% everywhere. The effects of tilt errors such as a linear instrumental bias across viewing angles was found to be more pronounced however, with the error in retrieved BRDF being on the same level as the tilt error. It therefore appears that random variations in instrumental gain do not affect the retrieval of BRDF to the degree that large-scale biases do.

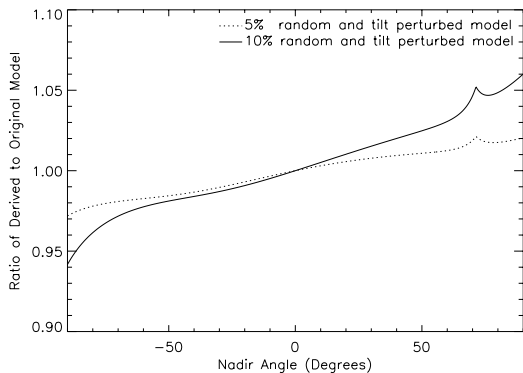


Figure 5: Ratio of derived Hapke model to original with 5% and 10% random and tilt error.

As seen in figure 3, the derived Hapke model differs from the original case for a 10% random error by less than 2.0% over all zenith angles in the principal plane of the derived model, which is the plane that showed the greatest deviation from unity. In the case of a 5% random error, this effect drops to less than 0.5%. Most notable in figure 3 is the blurring of the backscatter peak in the case of 10% error. The large error of 2% at view angles beyond the backscatter peak was caused by a ‘smearing’ of the peak into the BRDF continuum in the model. Similarly, in figure 4, the Walthall derived models show less than a 0.5% deviation from unity at all viewing angles for both the 5% and 10% random perturbed cases. This result was not surprising as the Walthall model does not incorporate the backscatter reflectance peak of the Hapke model, and is therefore less susceptible to scale random variations in the data.

The effect of a 5% and 10% random and tilt perturbation on the derived models were more pronounced in all cases than for just the random errors. Figure 5 and 6 show for the Hapke and Walthall derived models an error introduced of the same level as the tilt for both 5% and 10% cases respectively. Based on figure 6, the Walthall model appears to be more susceptible than the Hapke model to tilt errors, as the effect of the error is a non-linear change in the BRDF of the surface as a function of view angle. This is due to the fact that the Hapke model contains two linearity factors in its expression for BRDF while the Walthall model only has a single term to balance linearity.

Based on these results, it appears that the retrieval of BRDF functions by an instrument with a 10% random

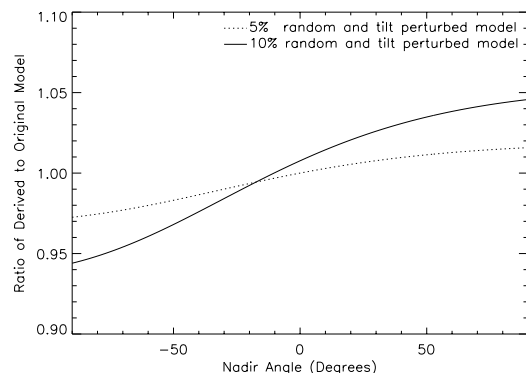


Figure 6: Ratio of derived Walthall model to original with 5% and 10% random and tilt error.

This result suggests that the calibration of instrument-wide characteristics (such as the lens function) of an imaging instrument has a greater impact on its overall performance for BRDF retrieval than the calibration of pixel-to-pixel gain variations.

The RSG is primarily interested in the vicarious calibration of Earth-observing satellite systems such as Landsat ETM+, therefore the level of the accuracy of BRDF retrieval required is driven by its effect on RTC calculated TOA radiance at the sensor on the satellite. To evaluate this effect, the original and perturbed Hapke and Walthall models derived above were used as inputs to the RSG's RTC and the change in output based on the models was examined.

4. EFFECT ON RADIATIVE TRANSFER

The radiative transfer model used in this study is a Gauss-Seidel iteration RTC.²⁷ This code has been used by the RSG to do reflectance-based vicarious calibration of satellites since the mid 1980s.²⁸ This RTC calculates TOA radiance by dividing the atmosphere into homogeneous plane-parallel layers based on the total optical thickness of the atmosphere. The horizontal distribution of scatterers is assumed to be homogenous and their vertical distribution is that of a modified 1976 U.S. Standard Atmosphere. Aerosols are assumed to be Mie scatterers and molecules are assumed to scatter as Rayleigh particles. This code allows for non-Lambertian surface types and can be provided a scattering phase function for a given surface to represent its BRDF.

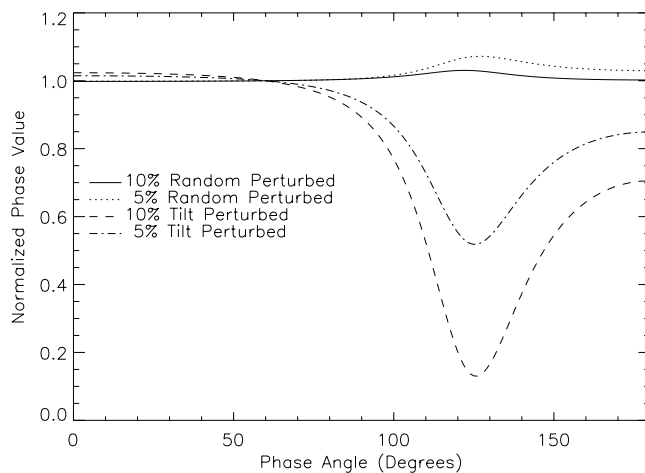


Figure 7: Ratio of perturbed model phase functions to original phase function for Hapke model cases. 0-degrees is the retro-reflection direction.

nadir-normalized in all cases. The ratio of each of the perturbed Hapke model's phase functions to the original model's phase function is shown in figure 7.

The Hapke model phases in general are within about 5% of the unperturbed phase value for phase angles between 0 and 80 degrees. A large deviation in the ratio between the perturbed and unperturbed cases occurs from 100 to 180 degrees in phase. This deviation is an artifact of the low specular reflection of this Hapke modeled surface, seen in figure 1 at -60 degrees. The low specular reflection component of the Hapke model makes the unperturbed phase very low at phase angles from 120-degrees to 180-degrees. This in turn makes the ratio of new versus old phase sensitive to slight changes in the perturbed phase, as seen in figure 7. This effect is dramatically exacerbated by the effects of the 5% and 10% tilt errors, which in this case reduced the specular reflection component of the Hapke model even further as can be seen from figure 5.

To evaluate the effect of BRDF retrieval errors on the calculation of TOA radiance, the Jacquemoud phase function was calculated for each of the ten model cases in this study. This was done by fitting the Jacquemoud phase function (2) after calculating the phase angles for each data point for each BRDF model. In the case of the Hapke models, the Jacquemoud phase function fit the data in all cases to better than 4.1% standard deviation. A new phase function was calculated for the original Hapke model and all four perturbed cases. Each phase function was normalized to its value at a phase angle of 60-degrees, which corresponds to a nadir viewing angle for a solar zenith of 60-degrees. This normalization was performed because the BRDF values used in this study will be

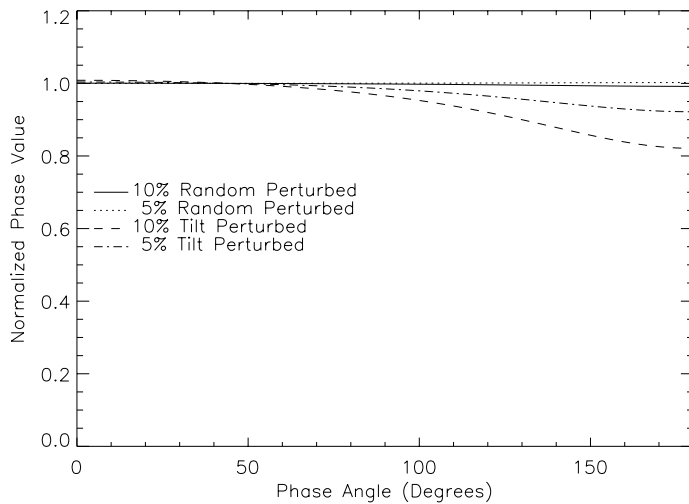


Figure 8: Ratio of perturbed model phase functions to original phase function for Walthall model cases. 0-degrees is the retro-reflection direction.

As with the Hapke model, it is clear that the deviation of phases from the 5% and 10% randomly perturbed models are less than those from the 5% and 10% random and tilt perturbed models.

The phase functions from the unperturbed and perturbed cases of both the Hapke and Walthall models were supplied to the RTC using atmospheric parameters consistent with those for a clear day appropriate for vicarious calibration activities. The aerosol optical depth was set to 0.119 and the molecular optical depth was set to 0.067. Results were computed at 538 and 550 nm wavelengths for the Hapke and Walthall model sets, with solar zenith angles of 60 and 44 degrees respectively and a surface reflectance value of 50%. In every case, the TOA radiance was calculated at view angles between -90 and 90 degrees, to simulate the view of a downward pointing satellite sensor. The TOA radiances from each of the perturbed model cases was ratioed against the TOA radiance reported from the unperturbed model case for both Hapke and Walthall models. As with figures 3 through 6, the greatest variations in TOA radiance were found in the principal planes, as shown in figures 9 and 10.

Figure 9 shows that the effects of 5% and 10% random errors in BRDF on the calculation of TOA radiance for a satellite sensor are negligible, less than 0.05% in all cases. The effect of a 10% tilt or instrumental bias effect on

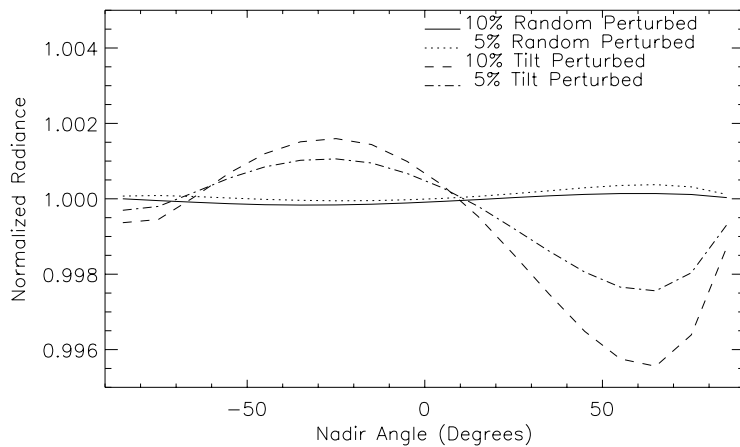


Figure 9: Ratio of perturbed model calculated TOA radiances to original model radiance for Hapke model cases. +60-degrees is the specular reflection direction.

Similarly, the Jacquemoud phase function was used to fit the Walthall model data to better than 0.6% standard deviation in all cases. Phase functions were calculated for each of the perturbed cases seen in figures 4 and 6, and were plotted as a ratio against the original model's unperturbed phase in figure 8. As can be seen, the greatest errors in phase produced by the perturbed models occurs at a phase angle of 180-degrees, outside the range of physical phase angles for this surface. Within the physical range of valid phase angles for the surface of 0 to 134 degrees, the errors are on the order of 15% for the 10% tilt case, 5% for the 5% tilt case, and less than 2% for the randomly-

the calculation of TOA is significantly greater, but in all cases is less than 0.4%, reaching that level only near the specular reflection region at +60 degrees viewing angle. Based on the very low reflectances expected at that angle from figure 1 and on the high proportional errors displayed in the phase function ratio of figure 7 this is an expected result. For the case of a 5% bias, the error in TOA radiance drops to less than 0.2% everywhere.

The ratio of the perturbed model - calculated TOA radiance to the original Walthall model was also calculated, and is shown in figure 10. As was true with the Hapke model cases, the errors resulting from the 5% and 10% randomly perturbed models are negligible, in all cases

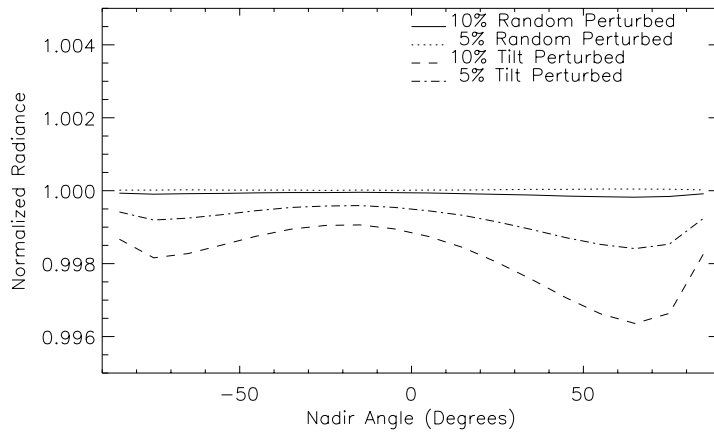


Figure 10: Ratio of perturbed model calculated TOA radiances to original model radiances for Walthall model cases. +44-degrees is the specular reflection direction.

under 0.05% for the unperturbed radiance. The errors from the 5% and 10% random and tilt perturbed cases are greater however, peaking at +70 degrees at a level of 0.4% for 10% error and 0.2% for the 5% tilt error case. The drop in overall radiance for the case of a 10% tilt is approximately 0.2% on average, down to less than 0.1% for the 5% tilted case. This is due primarily to the drop in phase value in these two cases at large phase angles, as is seen in figure 8. The lower average TOA radiance in these two cases is not surprising given they have on average lower phase values for phase angles greater than 50 degrees.

5. CONCLUSIONS

The BRDF of a surface was defined, and its relationship to measurable values was discussed. Two different BRDF models, the radiative-transfer derived Hapke model and the empirically-derived Walthall model were described and their parameters explained. These two models were then used to generate BRDFs based on soil surfaces consistent with those used by the RSG for vicarious calibration of satellites.

These models were then perturbed by various random and tilt errors to simulate the effect of the BRDFs being observed by a miscalibrated imaging instrument. The perturbed data sets were used to derive perturbed surface parameters which were used to generate new BRDF functions. These functions were compared against the originals to evaluate the effect of systemic errors on the retrieval of BRDF. In all cases, the effects of up to a 10% random error in the BRDF data produced less than a 0.2% effect in retrieved BRDF, while tilt errors produced errors on the same level as the tilt. Based on these results, errors in calibration that affect the across-array calibration of a BRDF imaging system (such as errors in the calibration of the lens function) have a much greater impact on BRDF retrieval than pixel-to-pixel gain variations.

To evaluate the effect of these perturbed BRDFs on the calculation of TOA radiance, the perturbed models were used to calculate phase functions, which were given to a Gauss-Seidel iterative RTC to calculate TOA radiance. These radiances were compared against the original, unperturbed radiance case to evaluate the impact of BRDF errors on the calculations. In all cases the errors generated by the tilt perturbed BRDFs were under 0.4%, and tended to occur near the specular reflectance peaks. These errors were much lower for cases of just random error, posing less than a 0.05% effect in all cases at all angles, for up to a 10% random error. Based on these results, it appears that the calculation of TOA radiance is insensitive to the effects of random errors in BRDF retrieval, but is moderately sensitive to system-bias type errors. To calculate TOA radiance to better than 0.1% therefore, tilt errors must be under 5% across the system, while pixel-to-pixel variations across an imaging detector can be as high as 10% without a significant impact on the retrieved radiance. Based on previous studies on the BRDF camera system by the RSG, this level of calibration was found to be achievable.¹⁸ It is therefore expected that CCD camera systems such as that of the RSGs will be able to retrieve BRDF data to the level required to improve the accuracy of vicarious calibration remote sensing methods for the calculation of TOA radiance. The RSG is currently investigating diffuse-light correction algorithms for the retrieval of BRDF data from camera data sets. It is expected that the inclusion of BRDF data into RTC calculations will improve the accuracy of calculated TOA radiances for vicarious calibration applications from 2-5% over certain field calibration sites.¹⁶

6. BIBLIOGRAPHY

1. B.Hapke, *Theory of Reflectance and Emittance Spectroscopy*, Cambridge University Press, p.333, 1993.
2. F.E.Nicodemus, J.C.Richmond, J.J.Hsia, "Geometrical Considerations and Nomenclature for Reflectance", National Bureau of Standards, October 1977.
3. S.R.Sandmeier, C.Muller, B.Hosgood, "Physical Mechanisms in Hyperspectral BRDF Data of Grass and Watercress", *Remote Sensing of the Environment*, **66**, pp.222-233, 1998.
4. D.W.Deering, T.F.Eck, B.Banerjee, "Characterization of the Reflectance Anisotropy of Three Boreal Forest Canopies in Spring-Summer", *Remote Sensing of the Environment*, **67**, pp.205-229, 1999.
5. B.Pinty, M.M.Verstraete, "On the Design and Validation of Surface Bidirectional Reflectance and Albedo Models", *Remote Sensing of the Environment*, **41**, pp.155-167, 1992.
6. W.Lucht, "Expected retrieval accuracies of bidirectional reflectance and albedo from EOS-MODIS and MISR angular sampling", *Journal of Geophysical Research*, **103**, pp.8763, April 27, 1998.
7. D.S.Kimes, "Dynamics of directional reflectance factor distributions for vegetation canopies", *Applied Optics*, **22(9)**, pp.1364-1372, 1983.
8. R.D.Jackson, P.M.Teillet, P.N.Slater, "Bidirectional Measurements of Surface Reflectances for View Angle Corrections of Oblique Imagery", *Remote Sensing of the Environment*, **32**, pp.189-200, 1990.
9. J.Roujean, "A Bidirectional Reflectance Model of the Earth's Surface for the Correction of Remote Sensing Data", *Journal of Geophysical Research*, **97(D18)**, pp.20,455-20,468, 1992.
10. D.M.O'Brien, "Estimation of BRDF from AVHRR Short-Wave Channels: Tests over Semiarid Australian Sites", *Remote Sensing of the Environment*, **66**, pp.71-86, 1998.
11. J.R.Dymond, C.M.Trotter, "Directional Reflectance of vegetation measured by a calibrated digital camera", *Applied Optics*, **36**, pp.4314-4318, June 1997.
12. A.I.Lyapustin, J.L.Privette, "A new method of retrieving surface bidirectional reflectance from ground measurements: Atmospheric sensitivity study", *Journal of Geophysical Research*, **104**, March 27, 1999.
13. K.J.Thome, "Proposed Atmospheric Correction for the Solar-Reflective Bands of the Advanced Spaceborne Thermal Emission and Reflection Radiometer", *IEEE*, pp.202-204, Feb. 1994.
14. W.C.Snyder, Z.Wan, Y.Zhang, Y.Feng, "Thermal Infrared (3-14um) Bidirectional Reflectance Measurements of Sands and Soils.", *Remote Sensing of the Environment*, **60**, pp.101-109, 1997.
15. L.Solheim, O.Engelsen, B.Hosgood, "Measurement and Modeling of the Spectral and Directional Reflection Properties of Lichen and Moss Canopies", *Remote Sensing of the Environment*, **v.72**, pp.78-94, 2000.
16. R.P.Santer, C.Schmechtig, K.J.Thome, "BRDF and surface-surround effects on SPOT-HRV vicarious calibration", *Proc EUROPTO*, 2960, pp.344-354, September 1996.
17. P.Nandy, K.Thome, S.Biggar, "Instrument for Retrieval of BRDF Data for Vicarious Calibration," *IEEE International Geoscience and Remote Sensing Symposium Proceedings (1998)*, Vol.2, pp.562-564.
18. P.Nandy, K.Thome, S.Biggar, "Characterization and field use of a CCD camera system for retrieval of bi-directional reflectance distribution function," *Journal of Geophysical Research*, 2000 (in publication).
19. P.Nandy, K.Thome, S.Biggar, "Laboratory characterization of a CCD camera system for retrieval of bi-directional reflectance distribution function," *Proc EUROPTO*, 3870, (1999).
20. J.R.Irons, G.S.Campbell, J.M.Norman, D.W.Graham, W.M.Kovalick, "Prediction and Measurement of Soil Bidirectional Reflectance", *IEEE Transactions on Geoscience and Remote Sensing*, **30**, pp.249-259, March 1992.
21. B.Hu, W.Lucht, X.Li, A.H.Strahler, "Validation of Kernel-Driven Semiempirical Models for the Surface Bidirectional Reflectance Distribution Function of Land Surfaces", *Remote Sensing of the Environment*, **62**, pp.201-214, 1997.
22. B.Pinty, M.M.Verstraete, R.E.Dickenson, "A physical model for predicting bidirectional reflectances over bare soil", *Remote Sensing of the Environment*, **27**, pp.272-288, 1989.
23. C.L. Walthall, J.M.Norman, J.M.Welles, G.Campbell, B.L.Blad, "Simple equation to approximate the bidirectional reflectance from vegetative canopies and bare soil surfaces", *Applied Optics*, **24**, pp.383-387, February 1985.
24. S. Jacquemoud, F.Baret, J.F.Hanocq, "Modeling Spectral and Bidirectional Soil Reflectance", *Remote Sensing of the Environment*, **41**, pp.123-132, 1992.

25. B.Hapke, "Bidirectional reflectance spectroscopy 1.Theory", Journal of Geophysical Research, 86(B4), pp.3039-3060, 1981.
26. S.Chandrasekhar, Radiative Transfer, Dover Publications, New York, 1960.
27. B.M. Herman, S.R.Browning, "A numerical solution to the equation of radiative transfer", Journal of Atmospheric Science, Vol. 22, pp2559-566, 1965.
28. P.N.Slater, S.F.Biggar, R.G.Holm et al., "Reflectance- and Radiance-based methods for the in-flight absolute calibration of multispectral sensors", Remote Sensing of the Environment, Vol.22, pp.11-37, 1987.